

Dependence of thermally stimulated current on the wavelength of the excitation light found in tetracene films

Takao Sakurai

Division of General Education, Ashikaga Institute of Technology, 268-1 Omae-cho, Ashikaga-shi, Tochigi 326, Japan

(Received 10 December 1990; revised manuscript received 29 October 1991)

A measurement is made of the thermally stimulated current (TSC), which is dependent on the wavelength of excitation light in vacuum-deposited tetracene films. The TSC curves are spectrally analyzed on the assumption that the TSC is caused not only by trapped holes but also by trapped charge-transfer (CT) excitons. Speculation on whether the same traps are responsible for the trapped holes and the trapped CT excitons is given.

I. INTRODUCTION

For experimental simplicity, the thermally stimulated current (TSC) and thermoluminescence (TL) methods have been extensively used to determine the trapping parameters of crystal imperfections.¹ However, these methods have not been fully explored. This is due to the observed TSC and TL curves being extremely complicated and not very accessible to a comprehensive analysis based on the fundamental model of TSC and TL, which has evolved from the first theoretical treatment by Randall and Wilkins.² The model commonly used consists of a single set of traps, with one trap located at a depth below the conduction band, while the other is located above the valence band. The traps within a given specimen are filled with trapped free carriers generated by photoexcitation at a low temperature. When the temperature of the specimen is raised, usually at a linear rate for convenience of analysis, these trapped carriers are freed and contribute to the excess current and/or luminescence. Therefore, the model predicts that the shapes of the TSC and TL spectra depend only on the probability of escape from the traps and not on the paths for filling the traps, namely the wavelength of the excited light, provided that the photoexcitation does not create any new damage to the specimen.

Actually, Yoshida *et al.*³ did not report a definite change in the TSC curves when an anthracene single crystal was excited by irradiated light of different wavelengths at various temperatures. Moreover, excitation spectra of the TL were found by Kristianpoller and Rehavi⁴ to be essentially identical for various TL peaks occurring in a ThO₂ single crystal. These results surely support the validity of the model. However, to the author's knowledge, there have been no observations of the TSC and TL curves dependent on the wavelength of the excitation light.

The purpose of the present paper is to show that the TSC curves are dependent on the wavelength of excitation light and to discuss the trapping mechanism responsible for the TSC in tetracene films. On the basis of the mechanism, the experimental TSC curves were spectrally analyzed.

II. EXPERIMENTAL PROCEDURE

A synthesized quartz plate was used as a substrate with Au being deposited on the quartz plate to form comb-type electrodes. The electrode separation was 1 mm. Tetracene refined through sublimation was deposited on the substrate at room temperature. As soon as a film was formed, it was cooled to 185 K. It was then irradiated by either 365- or 520-nm light. The light was supplied by a high-pressure 500-W Hg lamp, through bandpass glass filters having a half-width of 70 nm, under a bias voltage of 0 or 840 V. The former wavelength corresponds to the band-gap energy of a tetracene crystal,⁵ while the latter corresponds to the absorption of the 0-0 band in the lowest excited state of the crystal.^{6,7} The time of illumination, 5 min, was found sufficient for the traps to be saturated by photoexcitation. The film was then heated at a constant rate while the current through the film was measured. The current measurement was accomplished without changing the polarity of the applied voltage upon removal of the irradiation. It should be noted, however, that a field of reverse sign is applied in usual TSC measurements. It was confirmed, for the surface-type cells used here, that the TSC curves were not affected by the polarity of the collecting voltage. The evaporation and subsequent measurements were performed without exposing the films to air. The measured TSC spectra were found to depend on the conditions under which the film was formed, namely the film thickness, deposition rate, and the degree of vacuum. Moreover, when the film was annealed at room temperature after the measurement, the TSC no longer appeared.

III. RESULTS

A. Experimental TSC curves

Figures 1–3 show three TSC curves, dependent on the wavelength of the excitation light. These TSC curves were measured in three films formed under different conditions: in Fig. 1, the rather thick film was formed with a low deposition rate; in Fig. 2, the rather thin film was formed with a large deposition rate; in Fig. 3, the thin film was formed in a low degree of vacuum. Figures 1(a),

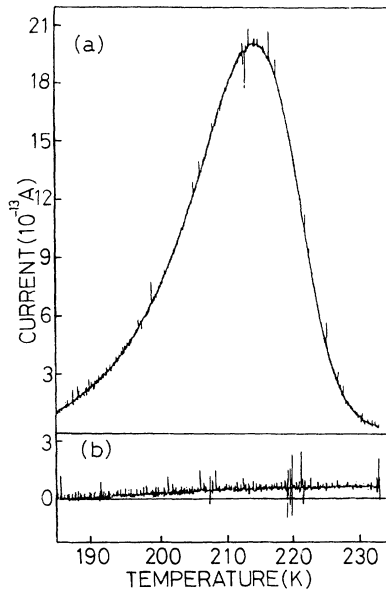


FIG. 1. TSC curves dependent on the wavelength of the excitation light. The conditions of the film formation are as follows: a thickness of $2.7 \times 10^3 \text{ \AA}$, deposition rate of 3 \AA/s , and degree of vacuum of $2.5 \times 10^{-5} \text{ Torr}$. The film was excited under 0 bias voltage. The heating rate was $5 \times 10^{-2} \text{ K/s}$.

2(a), and 3(a) show the TSC curves of films irradiated by 365-nm (3.4-eV) light at 185 K. After the TSC measurements were completed, the films were again cooled to 185 K through short circuiting of the electrodes. The TSC curves were then measured after the films were irradiated with 520-nm (2.4-eV) light. These TSC curves are shown in Figs. 1(b), 2(b), and 3(b).

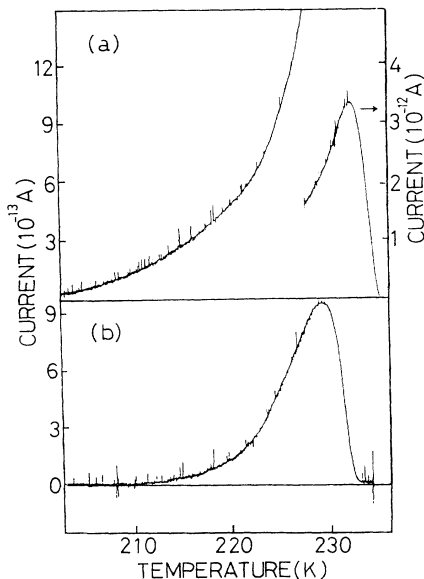


FIG. 2. As in Fig. 1 except for conditions as follows: a thickness of $1.8 \times 10^3 \text{ \AA}$, deposition rate of 5 \AA/s , and degree of vacuum of $1.8 \times 10^{-5} \text{ Torr}$. The heating rate was $3 \times 10^{-2} \text{ K/s}$.

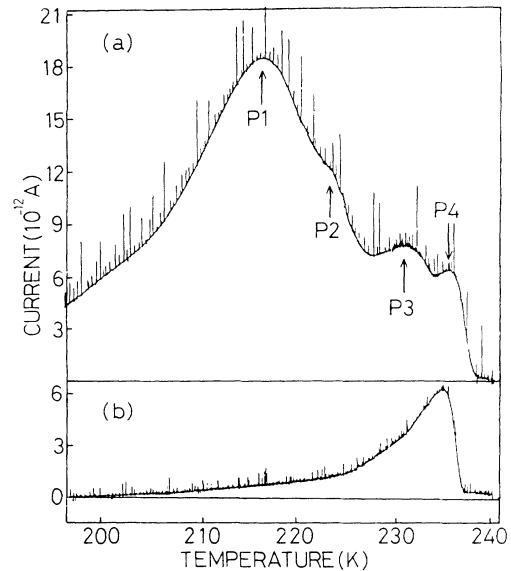


FIG. 3. As in Fig. 1 except for conditions as follows: a thickness of $1.6 \times 10^3 \text{ \AA}$, deposition rate of 4 \AA/s , and the degree of vacuum of $4.0 \times 10^{-5} \text{ Torr}$. The film was excited under a bias voltage of 840 V. The heating rate was $3 \times 10^{-2} \text{ K/s}$.

The broad TSC curve shown in Fig. 1(a) did not appear when the film was irradiated with 2.4-eV excitation [Fig. 1(b)]. The nonappearance is not due to any structural change in the film that may have been induced by repetition of the TSC measurement. It was confirmed that when the film was repeatedly excited by 3.4-eV light at low temperatures after the measurement of Fig. 1(b), the broad peak was still observed.

The half-width of the TSC curve shown in Fig. 1(a) is about 20 K, while those of the TSC curves shown in Fig. 2 are less than 10 K. The sharp TSC curve appeared even after film irradiation of 2.4-eV light as well as after the 3.4-eV excitation, although the values of the peak temperatures and peak currents differ between Figs. 2(a) and 2(b). The differences are probably due to structural changes in the film induced by repetitive TSC measurements. This was found to be true, since the film was again excited by the 3.4-eV light after the measurements of Fig. 2(b) were taken. The resulting TSC curve was similar to that of Fig. 2(b) in the current intensity and temperature of the TSC peak.

The more-complicated TSC curve shown in Fig. 3(a) consists of four peaks, which are indicated by arrows and labeled P1, P2, P3, and P4 in order of increasing temperature. Only one peak is found in Fig. 3(b). The large current that occurs as the temperature increases to approximately 217 K [Fig. 3(a)] is not observed in Fig. 3(b). However, the value of the peak current in Fig. 3(b) has the same order of magnitude as that of P4. It is evident that these differences are not due to the repetition of the TSC measurement. This conclusion was verified when the film was repeatedly excited by 3.4-eV light after the measurements of Fig. 3(b) were obtained, and TSC curves similar to that of Fig. 3(a) were found.

B. Spectral analysis

As shown in Fig. 4(a), the shape of the broad TSC curve shown in Fig. 1(a) was well fitted by the monomolecular TSC spectrum $I_1(T)$ (Refs. 2, 8, and 9) given by

$$I_1(T) = I_0 \exp \left[-\frac{E_t}{kT} - \frac{f}{B} \int_{T_0}^T \exp \left[-\frac{E_t}{kT} \right] dT \right]. \quad (1)$$

Here, k is the Boltzmann constant, f is the frequency factor for escape from the traps and is assumed to be independent of temperature T . B is the heating rate, I_0 is a constant dependent on the trap parameters, T_0 is the excitation temperature of the film, and E_t is the trap depth for free carriers. The solid lines (a) and (b) in Fig. 4 were computed by using Eq. (1). The values for E_t and f , given in the figure caption, were decided by a curve-fitting technique.¹⁰ The technique consisted of assuming a value of E_t , obtaining a value of f from the maximum condition of Eq. (1), calculating I_1 by Eq. (1), and comparing it graphically to the recorded graph. If the fit was not satisfactory, a different value of E_t was chosen, and the procedure was repeated until the best fit was obtained. In comparison with several previous results,¹¹⁻¹⁴ it is concluded that the broad TSC [Fig. 1(a)] originates from the thermal release of the holes at the trapping level, while the 2.4-eV excitation [Fig. 1(b)] cannot generate the trapped holes.

Nevertheless, the 2.4-eV excitation could fill traps responsible for the sharp TSC as well as the 3.4-eV excitation. The sharp TSC shown in Fig. 2(b) is not well fitted by Eq. (1), as shown in Fig. 4(b). The sharpening in the shape of the TSC does not arise from an arbitrary continuous distribution of traps.¹⁵ Hence, a new trapping mechanism and a corresponding TSC theory should be discussed. Recently, Sakurai¹⁶ demonstrated that the TSC curve $I(T)$ resulting from charge-transfer (CT) excitons trapped at a trap depth E can be expressed by

$$I(T) = \frac{I_0 \exp \left[-\frac{E+U}{kT} - \frac{F}{B} \int_{T_0}^T \exp \left[-\frac{E+U}{kT} \right] dT \right]}{1 + M \exp \left[-\frac{F}{B} \int_{T_0}^T \exp \left[-\frac{E+U}{kT} \right] dT \right]}. \quad (2)$$

Here U is the Coulombic binding energy between the electron and the hole, while F and M are assumed to be independent of T . The sharp TSC curve [Fig. 2(b)] was well fitted by Eq. (2), as shown in Fig. 5(b). Here, the curve-fitting technique was performed as mentioned above except for assuming a value of $E+U$ and a value of F independent of each other and obtaining a value of M from the maximum condition of Eq. (2). Consequently, the sharp TSC curve is most likely caused by the thermal release and dissociation of a trapped CT exciton. The trapped CT exciton consisting of a trapped hole with a free electron, or a trapped electron with a free hole as a nearest neighbor, was first proposed by Arnold, Pope, and Hisieh.¹⁷ However, the TSC curve shown in Fig. 2(a)

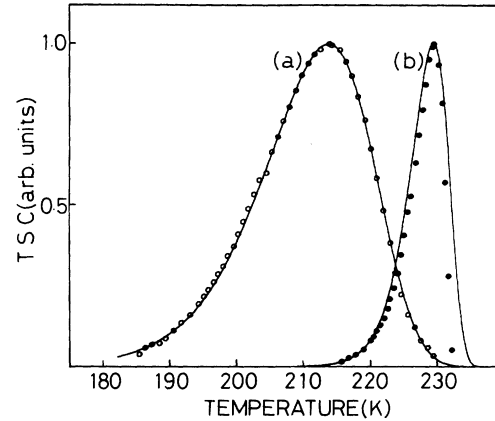


FIG. 4. Comparison of the theoretical TSC spectra with the experimental data of the broad and the sharp peaks shown in Figs. 1(a) and 2(b). The solid lines (a) and (b) are computed by using Eq. (1) with $E_t = 0.47$ eV and $f = 6.7 \times 10^8$ s⁻¹, and 1.6 eV and 1.3×10^{33} s⁻¹, respectively,

cannot be fitted by only one sharp TSC spectrum. This signifies that in Fig. 2(a) the broad TSC generated by the 3.4-eV excitation coexists with the sharp curve.

Maeta *et al.*^{18,19} theoretically proposed a method to separate parts of the TSC curve that overlap each other when they are subjected to Eq. (1). The procedure was applied to the present TSC data in the following manner. The data given when the current was increasing in Fig. 2(a) were subjected to Eq. (1) with the method of Maeta *et al.*, while the TSC data in the neighborhood of the peak were fitted to Eq. (2) independent of each other by the curve-fitting technique. The TSC curve resulting from the superposition of the two TSC spectra was compared to the experimental curve shown in Fig. 2(a).

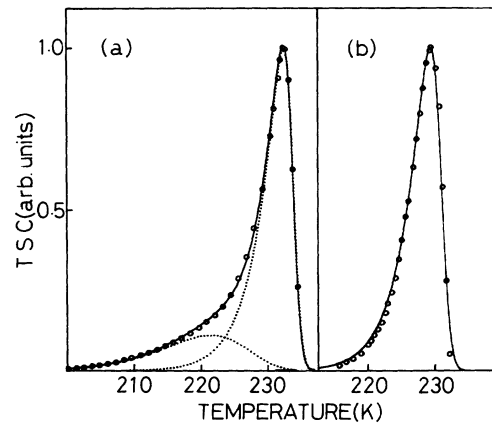


FIG. 5. Comparison of the theoretical TSC spectra with the experimental data shown in Fig. 2. Solid line (a) represents the superposition of two dotted lines that are computed by using Eq. (1) with $E_t = 0.65$ eV and $f = 2.8 \times 10^{12}$ s⁻¹, and Eq. (2) with $E+U = 1.28$ eV and $F = 1.9 \times 10^{26}$ s⁻¹. The solid line (b) is computed by using Eq. (2) with $E+U = 1.28$ eV and $F = 3.0 \times 10^{26}$ s⁻¹.

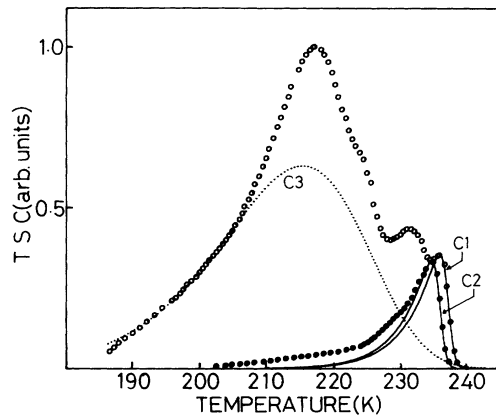


FIG. 6. Spectral fitting of the increasing and decreasing portions of the experimental data \circ and \bullet shown in Figs. 3(a) and 3(b), respectively. Curves C1 and C2 are computed by using Eq. (2), and curve C3 is computed by using Eq. (1).

These results were taken as trial values and the trial and error procedure was repeated until the best fit was obtained. The TSC curve was thus separated as shown in Fig. 5(a).

The increasing and decreasing portions of the TSC curves shown in Fig. 3 were also analyzed by the method mentioned above. The results are shown by the solid lines C1, C2, and dotted line C3 in Fig. 6. Using Eq. (2), curves C1 and C2 resulted from values of $E + U = 1.02$ eV, $F = 2.5 \times 10^{20} \text{ s}^{-1}$, and $M = 8.4 \times 10^3$, and 1.03 eV, $5.8 \times 10^{20} \text{ s}^{-1}$, and 8.2×10^3 , respectively. The three parameters, which characterize TSC curves caused by trapped CT excitons, appear to be the same for C1 and C2. Since the effect of overlapping other TSC signals on the parameters is negligible for C2 but not for C1, peak P4 was found to have a value of 1.03 eV for $E + U$ rather than 1.02 eV. In contrast, curve C3, calculated using Eq. (1), is due to the holes trapped at $E_t = 0.35$ eV. Since the effect of overlapping other TSC signals on curve C3 has a tendency to result in broadening the shape of C3, the value for E_t should be estimated as rather smaller than 0.35 eV.

IV. DISCUSSION

It is well known that the direct optical transition between the ground-state and CT exciton states is considered intermediate in the photogeneration process of free carriers.²⁰⁻²² On the basis of assumption that the band-gap energy is 3.4 eV, Sebastian, Weiser, and Bässler⁵ discovered four CT transitions at 2.71, 2.78, 2.90, and 3.06 eV in a tetracene polycrystalline film, corresponding to 0.69, 0.62, 0.50, and 0.34 eV for U , respectively. The appearance of the four peaks shown in Fig. 3(a) is thought to be consistent with the conclusion that the sharp TSC is caused by trapped CT excitons. If peak P4 is caused by the lowest CT exciton trapped at E , curve C1 yields a value of $E = 0.34$ eV because of $E + U = 1.03$

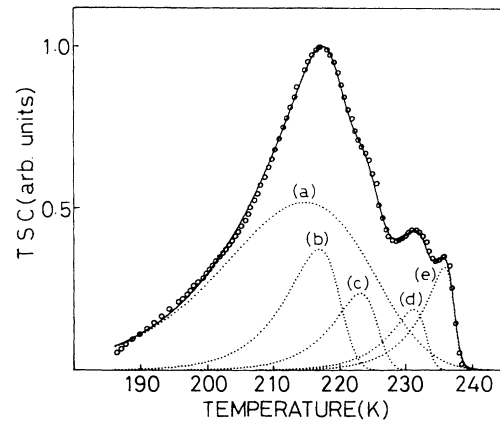


FIG. 7. Spectral fitting of the TSC curve shown in Fig. 3(a). Open circles are the experimental data. The dotted line (a) is computed by using Eq. (1) with $E_t = 0.34$ eV, and dotted lines (b)–(e) are computed by using Eq. (2) with $E = E_t$, $U = 0.34, 0.50, 0.62, \text{ and } 0.69$ eV, respectively. The solid line represents the superposition of curves (a)–(e).

eV and $U = 0.69$ eV. Therefore, it can be stated that the values for E and E_t precisely agree with each other. This is also supported by the result of spectral analysis shown in Fig. 5(a). This agreement signifies that the structural fault responsible for the hole traps is the same as that responsible for the CT exciton traps.

The trapped hole is thus interpreted as the trapped CT exciton with $U = 0$. In fact, Eq. (1) results from Eq. (2) on the condition that $U = 0$. The agreement further shows that it is reasonable to adopt the four values, derived from the four-CT transition found by Sebastian, Weiser, and Bässler,⁵ as the values for U of the trapped CT excitons. Consequently, it is concluded that the TSC curves shown in Figs. 3(a) and 3(b) can be interpreted by the superposition of five TSC curves as shown in Figs. 7 and 8, respectively. The TSC spectrum (a) in Fig. 8

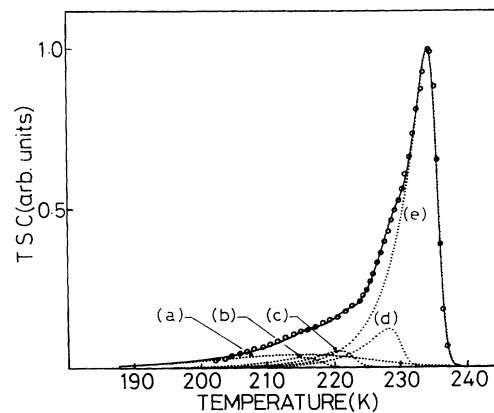


FIG. 8. Spectral fitting of the TSC curve shown in Fig. 3(b). The values of the parameters are the same as those given in Fig. 7.

caused by the trapped holes is thought to be due to the effect of the bias voltage.

It seems noteworthy to focus attention on the difference between the TSC spectra excited by the 3.4-eV and the 2.4-eV lights; the values of the four peak currents in Fig. 7 have the same order of magnitude, whereas in Fig. 8 a single peak appears. This is inconsistent with the assumption that the trapped CT exciton was generated by the trapped hole to capture a free electron from the nearest neighbor. It is expected, on the basis of the assumption, that the ratio of the peak values of the TSC spectra for the 2.4-eV excitation ought to be similar to that for the 3.4-eV excitation. Therefore, a direct optical CT transition should be considered as the generating mechanism of the trapped CT excitons for further interpretation of the remarkable difference between Figs. 7 and 8.

V. CONCLUSIONS

The complicated TSC curves, dependent on the wavelength of the excitation light, could be understood under the assumptions that the TSC is caused not only by trapped holes but also by trapped CT excitons, and that the trap depth of the trapped holes is equal to that of the trapped CT excitons. The 3.4-eV excitation was capable of simultaneously generating the trapped holes and CT excitons. However, the 2.4-eV excitation had the ability to generate the trapped CT excitons, but not the trapped holes under these experimental conditions.

ACKNOWLEDGMENTS

The author would like to express his thanks to Dr. S. Masuda for the purification of the tetracene and to Dr. S. H. Hayakawa for helpful discussions.

-
- ¹P. Bräunlich, P. Kelly, and J. P. Fillard, in *Thermally Stimulated Relaxation in Solids*, edited by P. Bräunlich (Springer-Verlag, Berlin, 1979).
- ²J. T. Randall and M. H. F. Wilkins, Proc. R. Soc. London, Ser. A **184**, 366 (1945).
- ³F. Yoshida, T. Akiyama, K. Fumoto, and S. Maeta, in *Proceeding of the Twenty-First Symposium on Electrical Insulating Materials* (Scientific Publishing Division of MYU K. K., Tokyo, 1988), pp. 291–294.
- ⁴N. Kristianpoller and A. Rehavi, Radiat. Eff. **72**, 209 (1983).
- ⁵L. Sebastian, G. Weiser, and H. Bässler, Chem. Phys. **61**, 125 (1981).
- ⁶T. Sakurai and S. Hayakawa, Jpn. J. Appl. Phys. **13**, 1733 (1974).
- ⁷R. Hesse, W. Hofberger, and H. Bässler, Chem. Phys. **49**, 201 (1980).
- ⁸R. R. Haering and E. N. Adams, Phys. Rev. **117**, 451 (1960).
- ⁹K. H. Nicholas and J. Woods, Br. J. Appl. Phys. **15**, 783 (1964).
- ¹⁰T. A. T. Cowell and J. Woods, Br. J. Appl. Phys. **18**, 1045 (1967).
- ¹¹G. Gamoudi, N. Rosenberg, G. Guillaud, M. Maitrot, and G. Mesnard, J. Phys. C **7**, 1149 (1974).
- ¹²G. M. Parkinson, J. M. Thomas, and J. O. Williams, J. Phys. C **7**, L310 (1974).
- ¹³A. Samoć, M. Samoć, J. Sworakowski, J. M. Thomas, and J. O. Williams, Phys. Status Solidi A **37**, 271 (1976).
- ¹⁴E. Eiermann, W. Hofberger, and H. Bässler, J. Non-Cryst. Solids **28**, 28 (1978).
- ¹⁵A. Samoć, M. Samoć, and J. Sworakowski, Phys. Status Solidi A **36**, 735 (1976).
- ¹⁶T. Sakurai, J. Phys. Soc. Jpn. **56**, 2866 (1987).
- ¹⁷S. Arnold, M. Pope, and T. K. T. Hisieh, Phys. Status Solidi B **94**, 263 (1979).
- ¹⁸S. Maeta and T. Akiyama, Trans. IEE Jpn. **109-A**, 83 (1989) (in Japanese).
- ¹⁹T. Akiyama, K. Fumoto, F. Yoshida, and S. Maeta, in *Proceeding of the Twenty-First Symposium on Electrical Insulating Materials* (Ref. 3), pp. 171–174.
- ²⁰R. R. Chance and C. L. Brauns, J. Chem. Phys. **64**, 3573 (1976).
- ²¹P. J. Bounds and W. Siebrand, Chem. Phys. Lett. **75**, 414 (1980).
- ²²L. Sebastian, G. Weiser, G. Peter, and H. Bässler, Chem. Phys. **75**, 103 (1983).